Photodimer of 9,10-Dimethylanthracene and Tetracene. Crystal and Molecular Structure, Photophysics, and Photochemistry

James Ferguson,*[1a] Albert W-H. Mau,[1b] and Peter O. Whimp[1c]

Contribution from the Research School of Chemistry, The Australian National University, Canberra, Australia. *Received February 3, 1978*

Abstract: The single-crystal X-ray analysis of the photodimer of 9,10-dimethylanthracene and tetracene is described. The dimer crystallizes in the monoclinic space group $P2_1/c$ with four molecules per unit cell of dimensions a = 21.323 (8) Å, b = 12.642 (4) Å, c = 8.587 (3) Å, and β = 93.25 (2)°. The conventional R factor for the 2573 reflections of the terminal data set for which $I/\sigma(I) \geq 3.0$ is 0.034. The bonds which are formed by the photodimerization [C(6)-C(26), 1.627 (2); C(13)-C(37), 1.629 (2) Å] are equal within experimental error. The molecular fluorescence is quenched by a thermally activated process, identified as a transfer of electronic excitation energy from the naphthalene chromophore into the pair of benzene chromophores in the other part of the molecule, followed by immediate photodissociation. The product molecules appear in their electronically excited (exciplex) state. Rephotodimerization of the dissociated molecules in the photodimer host crystal requires thermal activation. The polarization properties of the absorption and emission spectra of these dissociated molecules have been determined.

Bouas-Laurent and Castellan[2] reported the preparation of the mixed photodimer of 9,10-dimethylanthracene (DMA) and tetracene (T). This photodimer (DMA·T) raises the prospect of some very interesting spectroscopic and photochemical properties, by virtue of the naphthalene chromophore. In addition, photodissociation leads to the regeneration of the component molecules which can then be held in a sandwich arrangement by choice of the proper experimental conditions. One very important environment is that provided by the crystal of the photodimer and knowledge of its structure is an important ingredient in a spectral analysis.

The present paper reports a combined photochemical, photophysical, and crystallographic study of DMA·T. The spectroscopic properties of the photodissociated molecule (DMA + T) held in a sandwich arrangement are also included.

Experimental Section

The photodimer (DMA·T) was prepared according to the method of Bouas-Laurent and Castellan[2] by M. Puza. Crystals were grown from a dichloromethane–acetone mixed solvent.

Most of the spectroscopic methods have been described previously.[3,4] However, some consideration of the method used to detect and study the properties of excited state product emission is necessary. The basic technique has been described in outline.[4]

A Spex 1402 double monochromator was used to provide pure narrow band radiation and a double beam attachment was mounted at the exit slit. Two photomultipliers were used. One, in the double beam unit, detects the reference and sample signals and provides an optical density signal. The second is mounted on the sample compartment and views the luminescence at 90° to the incident beam. Cutoff filters and Polaroid sheet analyzers can be placed between the sample and this second photomultiplier to record excitation spectra, polarized if necessary. A feedback device, coupled to the first photomultiplier, adjusts the voltage of the second photomultiplier to maintain conditions corresponding to constant incident light intensity.

A solution of the pure photodimer, in a glass-forming solvent, was placed in a cold nitrogen or cold helium gas flow tube[4] passing vertically through the sample compartment and excitation spectra were measured at various temperatures, simultaneously with the absorption spectra. The very high sensitivity of the second photomultiplier (a cooled RCA C31034A) allows extremely small photon fluxes of exciting light to be used so that photodissociation of the photodimer is kept to a very low level. The eventual buildup of dissociated products can be detected easily by the appearance of their absorption bands in the excitation spectrum. Fluorescence excitation measurements are also made using vertically polarized exciting light and appropriate Polaroid analyzers to determine polarization ratios of the emitted fluorescence in rigid solvents.

In the present case the exciplex nature of the excited product emission was confirmed by replacing the second photomultiplier by a Spex 1704 monochromator, so that the spectral distribution could be determined under conditions of monochromatic excitation at a wavelength absorbed by the photodimer. Excitation spectra, with the wavelength of detection set at the exciplex intensity maximum, gave identical excitation spectra with those measured with the previous arrangement.

Time resolution (millisecond range) of the luminescence emission can be carried out using the rotating mirrors of the double beam unit as an effective phosphorescope. If triplet emission is present it can be detected using a boxcar averager.

X-ray Intensity Data Collection and Reduction. A suitable crystal was aligned in a random orientation on a Picker FACS-1 fully automatic four-circle diffractometer. Crystal data and data collection details are in Table I. Reflection intensities were reduced to values of $|F_o|$, and each reflection was assigned an individual estimated standard deviation. (The formulas used for data reduction and calculation of statistics are given in the section relating to computer programs, below). For this data set, the instrumental "uncertainty" factor[5] (ρ) was set at $(0.002)^{1/2}$. Reflection data were corrected for absorption effects,[6] equivalent reflection forms were averaged, and those reflections for which $I/\sigma(I) < 3.0$ were discarded as being unobserved. The statistical R factor (R_s) for the 2573 reflections of the terminal data set was 0.021.

Solution and Refinement of the Structure. The structure was solved by direct methods using the MULTAN[7] system of programs. Eight sets of signs for the 260 reflections with $|E| \geq 1.9$ were determined. The E map generated by the chosen starting set showed the positions of the 34 carbon atoms of the molecule. The structure was refined, initially by block-diagonal and, for the final cycles, by full-matrix least-squares methods to final unweighted and weighted R factors of 0.034 (R) and 0.037 (R_w), respectively. During least-squares refinement, the function minimized was $\Sigma w(|F_o| - |F_c|)^2$ and individual weights of the form $w = [\sigma(F_o)]^{-2}$ were used throughout; $R = \Sigma||F_o| - |F_c||/\Sigma|F_o|$; $Rw = \{\Sigma w[|F_o| - |F_c|]^2/\Sigma w|F_o|^2\}^{1/2}$; the anisotropic temperature factor was of the form $\exp[-(\beta_{11}h^2 + \beta_{22}k^2 + \beta_{33}l^2 + 2\beta_{12}hk + 2\beta_{13}hl + 2\beta_{23}kl)]$. The carbon atoms were refined with anisotropic temperature factors, and the hydrogen atoms, which were successfully refined, were assigned isotropic temperature factors. Atomic scattering factors for the carbon atoms were taken from the compilation of Cromer and Mann,[8] and were corrected for the real and imaginary parts of anomalous scattering.[9,10] Hydrogen atom scattering factors were taken from the compilation of Stewart et al.

On the final cycle of least-squares refinement, no individual parameter shift was greater than 0.05 of the corresponding parameter estimated standard deviation. The estimated standard deviation of

0002-7863/79/1501-2363$01.00/0

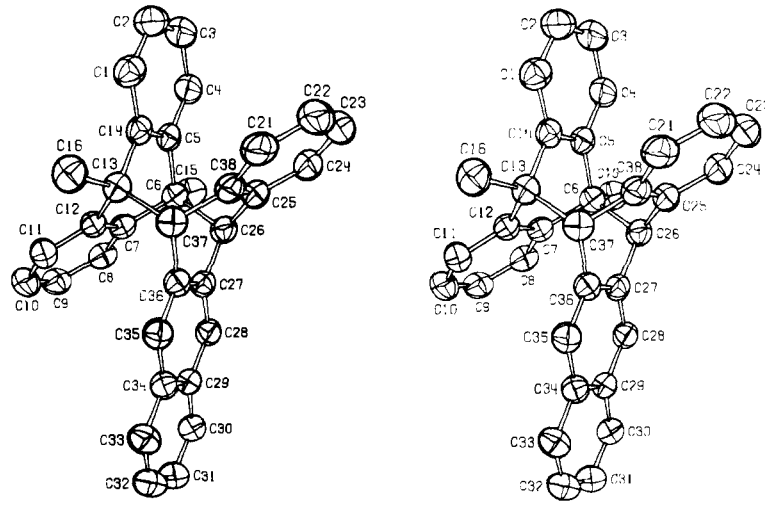

Figure 1. Perspective view of the photodimer (stereopair) showing the atom numbering sequence.

Table I. Crystal Data and Data Collection Details

radiation: Cu Kα	λ: 1.5418 Å
a = 21.323 (8) Å[a,b]	b = 12.642 (4) Å
c = 8.587 (3) Å	β = 93.25 (2)°
formula: $C_{34}H_{26}$	cell volume: 2311.0 Å^3
ρ_{obsd}: 1.24 (1) g cm^{-3}	ρ_{calcd}: 1.249 g cm^{-3}
μ (Cu Kα): 5.43 cm^{-1}	space group $P2_1/c$ [C_{2h}^5, no. 14]
monochromator: graphite crystal	crystal-counter distance: 28.5 cm
scan method and speed:	θ-2θ scans at 2°/min
scan width	from 0.85° below the Cu Kα_1 maximum to 0.85° above the Cu Kα_2 maximum
scan range	$3° \leq 2\theta \leq 125°$
total background count time[c]	20 s
"standard" reflections[d]	(940); ($\bar{1}$53); ($\bar{9}$40)
crystal decomposition	none
form of data collected[e]	hkl, $\bar{h}kl$, $h\bar{k}l$, $hk\bar{l}$, $\bar{h}\bar{k}l$, $\bar{h}k\bar{l}$, $h\bar{k}\bar{l}$
total number of data collected[e]	6939
number with $I/\sigma(I) \geq 3.0$	2573

[a] Cell dimensions were measured at 20 ± 1 °C. [b] Estimated standard deviations (in parentheses) in this and the following tables, and also in the text, refer to the least significant digit(s) in each case. [c] Backgrounds were measured on either "side" of each reflection (10 s each side) at the scan width limits, and were assumed to be linear between these two points. [d] The "standard" reflections were monitored after each 100 measurements throughout the course of data collection. [e] For statistical reasons, three independent data sets were collected. One set (hkl and $\bar{h}kl$) was collected in the range $3° \leq 2\theta \leq 125°$; the two remaining data sets were within the range $3° \leq 2\theta \leq 75°$.

an observation of unit weight, defined as $[\Sigma w(|F_o| - |F_c|)^2/(m - n)]^{1/2}$ [where m is the number of observations and n (= 412) is the number of parameters varied] was 1.65; cf. an expected value of 1.0 for ideal weighting. There were no unusual features on the final electron-density difference map, and there were no residual maxima greater than 0.15 e/Å^3. An extinction correction was applied,[12] and the extinction parameter, BO, refined successfully to $2.53 \times 10^{-5} \pm 1.6 \times 10^{-6}$. A weighting analysis showed that there was no serious dependence of the minimized function on either $|F_o|$ or $\lambda^{-1} \sin\theta$.

The final atomic positional and thermal parameters, together with their estimated standard deviations, are listed available as supplementary material only. A list of calculated and observed factor amplitudes [×10 (electrons)] is also available as supplementary material.

Computer Programs

All calculations were carried out on the Univac-1108 computer at The Australian National University Computer Centre, using the ANUCRYS system of programs. ANUCRYS is a system of crystallographic programs which has been implemented on the Univac-1108 computer by P. O. Whimp and D. Taylor, and contains programs from a variety of sources, as follows: DATSET, Picker diffractometer data tape translation with least-squares determination of the rate of decay of the "standard" reflections (D. Taylor and J. M. Rosalky, A. N. U.); SETUP3, data reduction,[13] correction for anisotropic crystal decomposition (if necessary),[14] and calculation of statistics[13] (P. O. Whimp); SORTER, sorting of reflection data together with averaging of multiple data observations (D. Taylor and P. O. Whimp); MULTAN, the 1974 version of the University of York direct methods package which includes programs for calculation of E values, assignment of phases, fast Fourier routine, peak search routine, and molecular fragment recognition[7]; BLKLSQ, a block-diagonal least-squares refinement program (4 × 4, or 3 × 3 and 6 × 6 matrices) based on Prewitt's SFLS-5[9] (locally modified by B. M. Foxman, P. O. Whimp, and D. Taylor); FULLSQ, a locally modified version (P. O. Whimp) of Prewitt's SFLS-5 full-matrix least-squares refinement program;[9] ANUFOR, a locally modified version (P. O. Whimp) of the University of Canterbury Fourier program; DANFIG, University of Canterbury lineprinter plotting program (based on ORTEP); HYDGEN, a locally modified version (D. Taylor and P. O. Whimp) of Hoppe's (UCLA) hydrogen atom generating program; TOMPAB, a locally modified version (J. D. Bell) of the Brookhaven National Laboratory absorption correction program;[15] ORTEP, Johnson's thermal ellipsoid plotting program;[16] ORFFE, the Oak Ridge National Laboratory program for calculation of errors;[17] LISTER, printout of final atomic parameters and esd's (D. Taylor); PUBTAB, printout of structure factor amplitudes (P. O. Whimp); MEANPL, calculation of weighted least-squares planes using the method described by Blow.[18]

Description and Discussion of the Structure

The crystal structure, as defined by the unit cell parameters, symmetry operations, and atom coordinates,[29] consists of discrete monomeric molecular units which have neither crystallographic nor virtual symmetry higher than C_1. There are no unusually short intermolecular contacts.

A perspective view of one molecule, together with the atom numbering scheme, is shown by the stereopairs of Figure 1, while the contents of one unit cell, as viewed down a^*, are shown by the stereopairs of Figure 2. In each figure, the thermal ellipsoids have been drawn to include 50% of the proba-

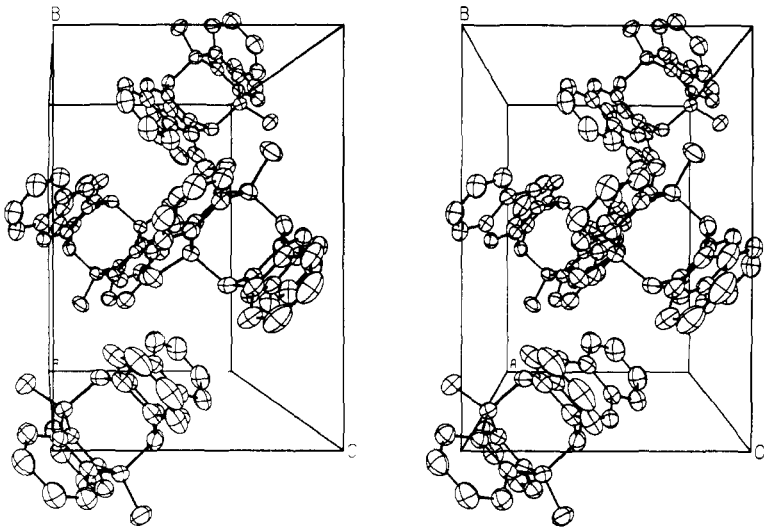

Figure 2. Stereoscopic view of one unit cell, viewed down a^*.

bility distribution, and, for clarity, the hydrogen atoms have been omitted.

Principal bond lengths and interbond angles, together with their estimated standard deviations, are listed in Table II. The results of least-squares planes calculations are collected in Table III.

The bonds which are formed by the photodimerization process [i.e., C(6)-C(26), 1.627 (2); C(13)-C(37), 1.629 (2) Å] are equal within experimental error (3.0σ), but are very much longer than the value of 1.537 (5) Å normally expected for simple carbon-carbon single bonds.[19a] Similarly long carbon-carbon distances have been found for the corresponding bonds in di-*p*-anthracene (1.62 Å),[20] and for the trans tetracene-tetracene photodimer [1.616 (3) Å].[21]

It is clear that, in each of these derivatives, there is considerable π-π repulsion between the two "halves" of each molecule. Although the distances between the centers of gravity of the two pairs of aromatic rings [i.e., 3.49 Å for the pair containing C(1) and C(21); 3.59 Å for the other pair] in the present derivative are in good agreement with the accepted van der Waals "thickness" of an aromatic ring (ca. 3.6 Å), the nonbonded distances immediately adjacent and parallel to the bonds formed by photodimerization [i.e., C(5)···C(25), 2.74; C(7)···C(27), 2.73; C(12)···C(36), 2.74; C(14)···C(38), 2.74 Å] are short and indicate considerable π-π interaction. Similar nonbonded distances (ca. 2.7-2.8 Å) have been found for a number of cyclophane derivatives[22] where the effects of π-π repulsion are relieved by the out of plane bending of the aromatic rings. In the present derivative, however, the effects of π-π repulsion are relieved by the abnormally long carbon-carbon single bonds, and the four "face to face" aromatic rings are planar within experimental error (Table III).

Using the energy minimization program described by Buckingham et al.,[23] and the appropriate force field potential function constants for bond length deformations,[23,24] bond angle deformations,[23,24] nonbonded interactions,[23] and torsional interactions,[23] we have calculated that the strain energy associated with the long carbon-carbon bonds [i.e., C(6)-C(26) and C(13)-C(37)] is 3.8 kcal mol^{-1} per bond for the refined crystallographic model. In addition, the strain energy associated with the short nonbonded carbon-carbon contacts mentioned above averages 1.0 kcal mol^{-1} per interaction.

Within the aromatic rings of this molecule, the geometry is normal. Thus, the C-C distances, which range from 1.361 (2) to 1.420 (2) Å, average 1.390 Å, while the internal C-C-C ring angles average 120.2°. In addition, the mean aromatic C-H distance is 1.00 Å, the average aromatic C-C-H angle is 119.7°, and the aromatic hydrogen atoms do not deviate significantly from their respective aromatic ring planes (Table III).

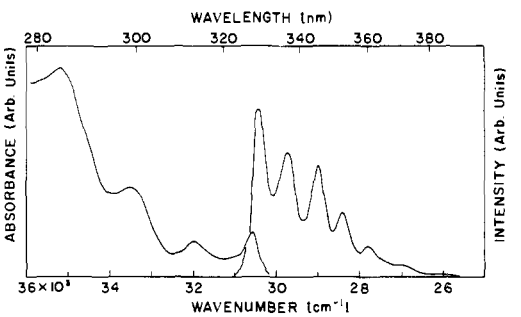

Figure 3. Absorption and fluorescence spectrum of DMA·T in methylcyclohexane at 77 K.

Apart from the long carbon-carbon distances which are formed by the photodimerization process and have been discussed above, the geometry within the (saturated) central ring system shows one other unusual feature. The four single carbon-carbon bonds [C(25)-C(26), 1.509 (2); C(26)-C(27), 1.511 (2); C(36)-C(37), 1.509 (2); C(37)-C(38), 1.507 (2) Å], equal within experimental error, are in excellent agreement with the value of 1.505 (5) Å normally expected for bonds between sp^2- and sp^3-hybridized carbon atoms.[19b] In contrast, the four remaining bonds [C(5) C(6), 1.530 (2); C(6)-C(7), 1.525 (2); C(12)-C(13), 1.531 (2); C(13)-C(14), 1.527 (7) Å], which are also equal within experimental error (average 1.528 Å), are significantly longer, and are only marginally shorter than the value of 1.537 (5) Å expected for bonds between two sp^3-hybridized carbon atoms.[19a] The two C-CH_3 distances [C(6)-C(15), 1.526 (2); C(13)-C(16), 1.530 (2) Å] are only slightly shorter than their expected value. Within this portion of the molecule, the C-C-C angles average 110.1°, and the C-H distances average 1.02 Å.

Photophysics and Photochemistry of DMA·T in Solution

The absorption spectrum of DMA·T is dominated by the naphthalene chromophore, being very similar to the spectrum of 2,3-dimethylnaphthalene. In contrast, it might be expected that excited-state (exciplex) interaction between the naphthalene and its facing benzene chromophore (see Figure 1) would modify, in some way, the fluorescence spectrum. However, the fluorescence spectrum (Figure 3) shows no evi-

Table II. Bond Lengths and Interbond Angles

A. Bond Lengths, Å

atoms	distance	atoms	distance	atoms	distance
C(1)-C(2)	1.377 (2)	C(1)-C(14)	1.388 (2)	C(2)-C(3)	1.368 (2)
C(3)-C(4)	1.380 (2)	C(4)-C(5)	1.396 (2)	C(5)-C(14)	1.400 (2)
C(7)-C(8)	1.398 (2)	C(7)-C(12)	1.400 (2)	C(8)-C(9)	1.374 (2)
C(9)-C(10)	1.375 (2)	C(10)-C(11)	1.383 (2)	C(11)-C(12)	1.386 (2)
C(21)-C(22)	1.380 (3)	C(21)-C(38)	1.392 (2)	C(22)-C(23)	1.381 (3)
C(23)-C(24)	1.388 (3)	C(24)-C(25)	1.392 (2)	C(25)-C(38)	1.388 (3)
C(27)-C(28)	1.365 (2)	C(27)-C(36)	1.416 (2)	C(28)-C(29)	1.415 (2)
C(29)-C(30)	1.415 (2)	C(29)-C(34)	1.420 (2)	C(30)-C(31)	1.363 (2)
C(31)-C(32)	1.397 (3)	C(32)-C(33)	1.361 (2)	C(33)-C(34)	1.419 (2)
C(34)-C(35)	1.418 (2)	C(35)-C(36)	1.361 (2)		
C(5)-C(6)	1.530 (2)	C(6)-C(7)	1.525 (2)	C(6)-C(15)	1.526 (2)
C(12)-C(13)	1.531 (2)	C(13)-C(14)	1.527 (7)	C(13)-C(16)	1.530 (2)
C(25)-C(26)	1.509 (2)	C(26)-C(27)	1.511 (2)	C(36)-C(37)	1.509 (2)
C(37)-C(38)	1.507 (2)				
C(6)-C(26)	1.627 (2)	C(13)-C(37)	1.629 (2)		
C(1)-H(1)	0.95 (1)	C(2)-H(2)	0.97 (2)	C(3)-H(3)	1.02 (1)
C(4)-H(4)	1.00 (1)	C(8)-H(8)	1.02 (2)	C(9)-H(9)	0.98 (2)
C(10)-H(10)	1.02 (1)	C(11)-H(11)	0.99 (1)	C(15)-H(15A)	1.00 (2)
C(15)-H(15B)	1.00 (2)	C(15)-H(15C)	1.03 (2)	C(16)-H(16A)	1.02 (2)
C(16)-H(16B)	1.00 (2)	C(16)-H(16C)	1.02 (1)	C(21)-H(21)	1.01 (2)
C(22)-H(22)	1.00 (2)	C(23)-H(23)	1.03 (2)	C(24)-H(24)	1.04 (2)
C(26)-H(26)	1.02 (1)	C(28)-H(28)	1.02 (1)	C(30)-H(30)	1.00 (1)
C(31)-H(31)	1.02 (2)	C(32)-H(32)	1.01 (2)	C(33)-H(33)	1.01 (2)
C(35)-H(35)	0.98 (1)	C(37)-H(37)	1.03 (1)		

B. Interbond Angles, deg

atoms	angle	atoms	angle	atoms	angle
C(14)-C(1)-C(2)	121.2 (2)	C(1)-C(2)-C(3)	120.1 (2)	C(2)-C(3)-C(4)	119.9 (2)
C(3)-C(4)-C(5)	121.0 (2)	C(4)-C(5)-C(6)	122.7 (1)	C(4)-C(5)-C(14)	118.7 (1)
C(14)-C(5)-C(6)	118.6 (1)	C(6)-C(7)-C(8)	122.6 (1)	C(6)-C(7)-C(12)	118.6 (1)
C(12)-C(7)-C(8)	118.8 (1)	C(7)-C(8)-C(9)	121.1 (2)	C(8)-C(9)-C(10)	120.2 (2)
C(9)-C(10)-C(11)	119.5 (2)	C(10)-C(11)-C(12)	121.2 (2)	C(11)-C(12)-C(13)	122.6 (1)
C(11)-C(12)-C(7)	119.2 (1)	C(7)-C(12)-C(13)	118.2 (1)	C(13)-C(14)-C(1)	122.8 (1)
C(13)-C(14)-C(5)	118.1 (1)	C(5)-C(14)-C(1)	119.1 (1)	C(38)-C(21)-C(22)	120.0 (2)
C(21)-C(22)-C(23)	120.6 (2)	C(22)-C(23)-C(24)	120.0 (2)	C(23)-C(24)-C(25)	119.8 (2)
C(24)-C(25)-C(26)	123.3 (2)	C(24)-C(25)-C(38)	120.0 (2)	C(38)-C(25)-C(26)	116.7 (1)
C(26)-C(27)-C(28)	123.1 (1)	C(26)-C(27)-C(36)	116.8 (1)	C(36)-C(27)-C(28)	120.1 (1)
C(27)-C(28)-C(29)	121.2 (2)	C(28)-C(29)-C(30)	122.5 (2)	C(28)-C(29)-C(34)	118.6 (1)
C(34)-C(29)-C(30)	118.8 (1)	C(29)-C(30)-C(31)	121.0 (2)	C(30)-C(31)-C(32)	120.0 (2)
C(31)-C(32)-C(33)	120.9 (2)	C(32)-C(33)-C(34)	120.7 (2)	C(33)-C(34)-C(35)	122.7 (2)
C(33)-C(34)-C(29)	118.4 (2)	C(29)-C(34)-C(35)	118.9 (1)	C(34)-C(35)-C(36)	121.1 (2)
C(35)-C(36)-C(37)	123.8 (1)	C(35)-C(36)-C(27)	120.1 (1)	C(27)-C(36)-C(37)	116.1 (1)
C(37)-C(38)-C(21)	123.1 (2)	C(37)-C(38)-C(25)	117.3 (1)	C(25)-C(38)-C(21)	119.6 (2)
C(5)-C(6)-C(7)	106.8 (1)	C(5)-C(6)-C(26)	110.8 (1)	C(5)-C(6)-C(15)	111.7 (1)
C(7)-C(6)-C(15)	111.8 (1)	C(7)-C(6)-C(26)	109.7 (1)	C(15)-C(6)-C(26)	105.2 (1)
C(12)-C(13)-C(14)	106.6 (1)	C(12)-C(13)-C(37)	110.7 (1)	C(12)-C(13)-C(16)	111.4 (1)
C(14)-C(13)-C(16)	112.1 (1)	C(14)-C(13)-C(37)	110.2 (1)	C(16)-C(13)-C(37)	105.9 (1)
C(25)-C(26)-C(27)	108.8 (1)	C(25)-C(26)-C(6)	111.9 (1)	C(27)-C(26)-C(6)	112.7 (1)
C(36)-C(37)-C(38)	109.1 (1)	C(36)-C(37)-C(13)	112.0 (1)	C(38)-C(37)-C(13)	112.7 (1)

dence of this and it is also very similar to the spectrum of 2,3-dimethylnaphthalene.

The significant property of the fluorescence is its temperature-dependent quenching, shown in Figure 4, in which the limiting low-temperature yield is assumed to be unity. Making the further assumption that the quenching is due to a thermally activated photodissociation rate ($k_d = A \exp(-E^{\ddagger}/KT)$) an Arrhenius plot (Figure 5) provides the following parameters: $A = 7.2 \times 10^{15}\ s^{-1}$, $E^{\ddagger} = 4.15 \times 10^3\ cm^{-1}$. The quenching parameters are the same in the much more viscous solvent methylcyclohexane-decalin (1:1) so, very probably, they are intrinsic.

The activation barrier is large and, assuming it is intrinsic, we add it to the purely electronic fluorescent energy (30 600 cm^{-1}) to obtain 34 750 cm^{-1} (288 nm). This is just the expected energy of the lowest singlet excited state of the pair of facing benzene chromophore groups in the molecule. It seems likely therefore that the activation barrier can be ascribed to the energy difference between the naphthalene and benzene chromophores in the molecule.

Electronic excitation energy localized in this region of the molecule can then follow a pathway analogous to that in dianthracene and related compounds, as was shown recently.[25] All of these compounds give rise to excited-state (excimer or exciplex) products in surprisingly high yield at lower temperatures, below about 200 K, for which the quenching photodimerization or photoisomerization reaction yield is nearly zero.

Exciplex fluorescence was therefore looked for and found (see Experimental Section). It has the same intensity distribution as the emission from the sandwich pair in the photoisomer crystal (see Figure 7). This emission was then monitored with the arrangement described above and a series of excitation spectra measured as a function of temperature. The intensity of this emission is strongly dependent on temperature. These measurements also show that there is a very weak tem-

Table III. Least-Squares Planes

A. Best Weighted Least-Squares Planes

plane	atoms defining plane	equation[a]
1	C(1), C(2), C(3), C(4), C(5), C(14)	$0.4292X - 0.6887Y - 0.5844Z + 6.3532 = 0$
2	C(7), C(8), C(9), C(10), C(11), C(12)	$-0.3563X - 0.5550Y - 0.7517Z + 18.5379 = 0$
3	C(1), C(22), C(23), C(24), C(25), C(38)	$-0.3609X - 0.5875Y - 0.7243 + 17.3162 = 0$
4	C(27), C(28), C(29), C(34), C(35), C(36)	$0.4282X - 0.6512Y - 0.6265 + 4.6724 = 0$
5	C(29), C(30), C(31), C(32), C(33), C(34)	$0.4181X - 0.6357Y - 0.6489 + 4.7212 = 0$
6	C(26), C(27), C(28), C(29), C(30), C(31) C(32), C(33), C(34), C(35), C(36), C(37)	$0.4258X - 0.6512Y - 0.6282 + 4.7229 = 0$

B. Deviations (Å) of Atoms from Mean Planes

atom	plane 1	atom	plane 2	atom	plane 3
C(1)	0.000 (2)	C(7)	0.003 (1)	C(21)	−0.003 (2)
C(2)	−0.005 (2)	C(8)	0.002 (2)	C(22)	−0.004 (2)
C(3)	0.004 (2)	C(9)	−0.005 (2)	C(23)	0.005 (2)
C(4)	0.003 (2)	C(10)	0.001 (2)	C(24)	0.001 (2)
C(5)	−0.005 (1)	C(11)	0.005 (2)	C(25)	−0.005 (2)
C(14)	0.004 (1)	C(12)	−0.005 (1)	C(38)	0.005 (2)
C(6)	−0.036 (1)	C(6)	0.027 (1)	C(26)	−0.056 (2)
C(13)	0.036 (1)	C(13)	−0.008 (1)	C(37)	0.010 (2)
H(1)	−0.02 (1)	H(8)	0.04 (2)	H(21)	−0.04 (2)
H(2)	0.04 (2)	H(9)	0.01 (2)	H(22)	0.02 (2)
H(3)	0.02 (2)	H(10)	0.01 (1)	H(23)	0.06 (2)
H(4)	−0.03 (1)	H(11)	0.02 (1)	H(24)	−0.02 (2)
atom	plane 4	atom	plane 5	atom	plane 6
C(27)	0.005 (1)	C(29)	0.008 (2)	C(26)	0.015 (2)
C(28)	0.004 (2)	C(30)	0.001 (2)	C(27)	0.012 (1)
C(29)	−0.009 (2)	C(31)	−0.011 (2)	C(28)	0.014 (2)
C(34)	0.007 (2)	C(32)	0.006 (2)	C(29)	0.005 (2)
C(35)	0.002 (2)	C(33)	0.008 (2)	C(30)	−0.034 (2)
C(36)	−0.007 (1)	C(34)	−0.011 (2)	C(31)	−0.047 (2)
C(26)	0.011 (2)	C(27)	−0.019	C(32)	0.004 (2)
C(30)	−0.052 (2)	C(28)	0.016 (2)	C(33)	0.038 (2)
C(31)	−0.067 (2)	C(35)	−0.052 (2)	C(34)	0.020 (2)
C(32)	−0.016 (2)	C(36)	−0.064 (1)	C(35)	0.011 (2)
C(33)	0.022 (2)	H(30)	−0.04 (2)	C(36)	−0.001 (1)
C(37)	−0.047 (2)	H(31)	−0.08 (2)	C(37)	−0.046 (2)
H(28)	0.01 (1)	H(32)	−0.02 (2)	H(28)	0.02 (1)
H(35)	−0.02 (1)	H(33)	−0.05 (2)	H(30)	−0.10 (1)
				H(31)	−0.14 (2)
				H(32)	−0.03 (2)
				H(33)	0.00 (2)
				H(34)	−0.01 (1)

[a] The plane equations $LX + MY + NZ + D = 0$ refer to orthogonal coordinates where $X = 21.3233x + 0.0y - 0.4864z$; $Y = 0.0x + 12.6417y + 0.0z$; $Z = 0.0x + 0.0y + 8.5730z$.

perature-independent exciplex emission (below about 240 K) in addition to the much more intense temperature-dependent emission which appears at about 240 K. The appearance of this latter emission is coincident with the onset of the quenching of the fluorescence from the naphthalene chromophore (see Figure 4). We conclude therefore that the temperature-dependent exciplex emission is good evidence for the thermally activated mechanism postulated above, i.e., a thermal transfer of electronic excitation energy from the naphthalene chromophore into the pair of facing benzene chromophores.

The temperature-independent photodissociation has a very low apparent quantum yield and there are probably two different mechanisms involved. In one, the excitation occurs initially in the pair of benzene chromophores which are face to face and photodissociation follows immediately. In the other, the initial more probable absorption is localized in the naphthalene chromophore and very fast relaxation to the lowest electronic energy level near 30 600 cm^{-1} takes place. At this point, probably because of the absence of significant charge-transfer interaction between the naphthalene and the facing benzene chromophore, the probability of a radiationless relaxation to the dissociated state is greatly reduced, so that fluorescence is observed with high efficiency. Photodissociation does occur, but with a very small (undetermined) yield. There is some evidence which suggests that wavelengths less than about 290 nm have a relatively higher photodissociation quantum yield than wavelengths greater than this figure, corresponding to the first mechanism, but an experimental discrimination between the two mechanisms is difficult to carry out. No long-lived (triplets) emission could be detected in any of these experiments.

Photophysics of Dissociated DMA·T at 77 K

Irradiation of DMA·T in methylcyclohexane at 77 K leads to photodissociation and the production of the component molecules held in a sandwich arrangement by the constraints of the rigid glass. The corresponding absorption and emission spectra are given in Figure 6A and the spectra of the dissociated molecules are in Figure 6B.

Contrary to expectation the fluorescence of the sandwich pair does not show the structureless emission band of an exciplex. Rather it is similar to partially relaxed dimer fluorescence observed earlier for sandwich dimers after slight softening.[26] The experiments were therefore repeated with the glassy ma-

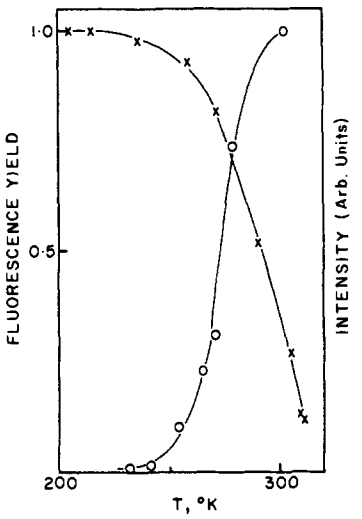

Figure 4. Fluorescence yield of DMA·T as a function of temperature in methylcyclohexane-isopentane (1:3) (x—x—x). Exciplex fluorescence intensity (arbitrary units) as function of temperature (O—O—O). Excitation wavelength for both measurements was 284 nm.

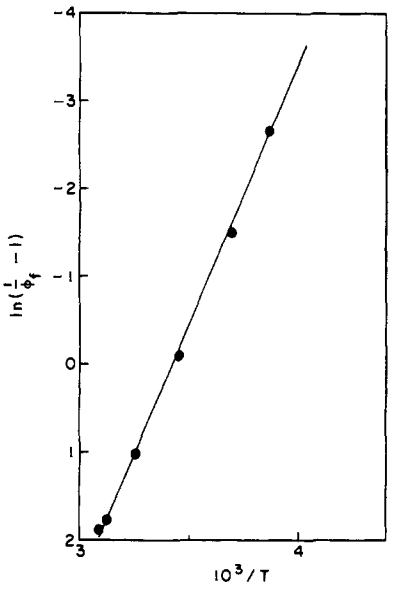

Figure 5. Arrhenius plot of the fluorescence quenching of DMA·T (Figure 4).

trix at 10 K but essentially similar spectra were obtained. Unlike the case with the photoisomer of 1-(9-anthryl)-3-(1-naphthyl)propane,[27] where there is a constraining bridge, it appears that photodissociation leads to a range of conformations with overlapping fluorescence spectra.

Photophysics and Photochemistry of DMA·T Single Crystals

The well-developed face of the crystals is (100), and the molecular orientation with respect to this face is shown by the stereopairs of Figure 2. Intense emission from the lowest absorption band is easily observed (Figure 7). There appears to be both intrinsic and defect emission, the latter denoted by X in Figure 7.

An oriented gas model gives for the orientation of the naphthalene chromophore in the crystals an expected polarization ratio (c/b) of 6.6:1 if the transition moment direction lies along the long axis of the naphthalene chromophore. The

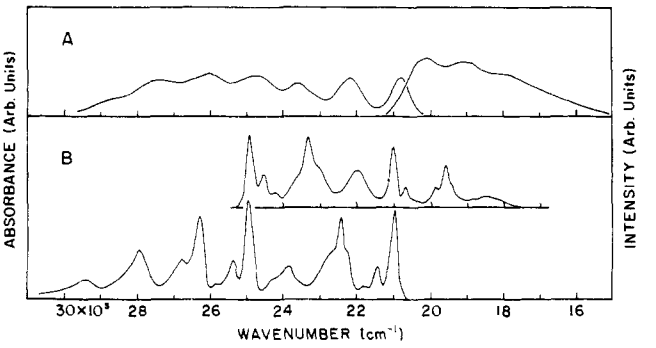

Figure 6. (A) Absorption spectrum of photodissociated DMA·T in a methylcyclohexane glass at 77 K (left curve) and fluorescence spectrum excited by 400-nm light (right curve). (B) Absorption spectrum of photodissociated DMA·T at 77 K after allowing softening of the glass to occur (lower curves) and corresponding fluorescence spectrum excited by 270-nm light (upper curve).

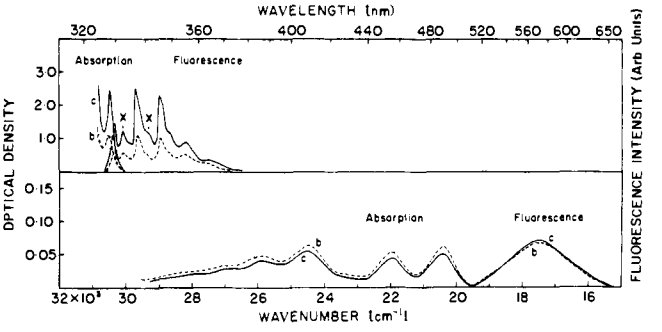

Figure 7. Upper panel: polarized absorption and fluorescence spectra of DMA·T for light normal to the well-developed (100) face at 10 K. Lower panel: absorption (left of 19 500 cm^{-1}) and fluorescence (right of 19 500 cm^{-1}) spectra (at 10 K) of a single DMA·T crystal, light normal to (100) face, after room temperature irradiation with 254-nm light.

observed ratio is 2/1 in absorption and a little higher in emission. The actual site symmetry in the crystal allows a mixing of short and long axis polarized transitions so the reduction from the oriented gas ratio is not surprising.

Prolonged irradiation of a crystal of DMA·T at 10 K with 254-nm light leads to an extremely small yield of photodissociated molecules together with other unidentified photoproducts, unlike the analogous experiments with glassy solutions. The photodissociation is effectively quenched in the crystal at low temperatures for reasons which are not understood.

On the other hand, irradiation of the crystal at room temperature does lead to photodissociation and the polarized absorption and emission spectra of the product, measured at 10 K, are given in Figure 7. In this case the absorption spectrum shows only a small anisotropy with a ratio b/c of about 1.1:1. Assuming no rotation of the dissociated components, following cleavage, we estimate a polarization ratio $b/c = 1.2$ for a short axis polarized transition in either DMA or T. The emission spectrum shows even less anisotropy, with the c polarization perhaps marginally greater in its intensity. We conclude from this that the exciplex emission spectrum is essentially short axis polarized, with respect to the two component molecules, but it is likely that there is a component which is in a direction normal to these planes. The latter would explain the small polarization difference between the absorption and emission spectra. It is the expected[28] charge-transfer component of the exciplex transition moment, but the orientation of the molecules in the crystal is not a favorable one to distinguish between vectors normal to the molecule planes and their short axis vector directions.

Table IV. Fluorescence Lifetimes (ns)

species	medium	
	MCH 77 K	crystal
DMA·T	95	80
(DMA + T)[a]	60	85
DMA	13	
T	8.5	

[a] (DMA + T) signifies photodissociated molecule, constrained by the environment in a "sandwich" geometry.

The exciplex character of the emission is in contrast to the fluorescence obtained after photodissociation in glassy solvents. The DMA·T host crystal provides a greater constraint for the dissociated fragment molecules so that excitation leads to an exciplex state. However, the conformation is not topochemical in terms of the photodimerization pathway, which is followed only as a result of thermal activation. The exciplex emission intensity is independent of temperature below about 150 K, while it is quenched above this value and photodimerization proceeds.

Fluorescence Decay Times. The fluorescence decay times were measured using dye laser excitation and the values are given in Table IV.

Acknowledgments. We are grateful for generous allocations of time on the Univac-1108 computer at The Australian National University Computer Centre.

Supplementary Material Available: A listing of structure factor amplitudes (13 pages). Ordering information is given on any current masthead page.

References and Notes

(1) (a) Research School of Chemistry, The Australian National University. (b) Division of Applied Organic Chemistry, C.S.I.R.O., P.O. Box 4331, G.P.O., Melbourne, Victoria 3001, Australia. (c) Physics & Engineering Laboratory, D.S.I.R., Lower Hutt, New Zealand.
(2) H. Bouas-Laurent and A. Castellan, *Chem. Commun.*, 1648–1659 (1970).
(3) J. Ferguson and A. W-H. Mau, *Mol. Phys.*, **27**, 377–387 (1974).
(4) J. Ferguson, *Spex Speaker XXI*, **No. 1** (1976).
(5) W. R. Busing and H. A. Levy, *J. Chem. Phys.*, **26**, 563–568 (1957); P. W. R. Corfield, R. J. Doedens, and J. A. Ibers, *Inorg. Chem.*, **6**, 197–204 (1967).
(6) The crystal used for data collection was bounded by the faces {100}, {100}, {111}, {111}, {111}, and {111}. Crystal dimensions follow: {100} to {100}, 0.0125 cm; {111} to {111}, 0.020 cm; {111} to {111}, 0.025 cm. Transmission factors (which were applied to $|F_o|$) ranged from 0.940 to 0.970.
(7) MULTAN74 is the 1974 version of the University of York direct methods package of programs written and assembled by P. Main, M. M. Woolfson, L. Lessinger, G. Germain, and J-P. Declercq.
(8) D. T. Cromer and J. B. Mann, *Acta Crystallogr., Sect. A*, **24**, 321–324 (1968).
(9) C. T. Prewitt, Ph.D. Thesis, Massachusetts Institute of Technology, 1962, p 163.
(10) D. T. Cromer and D. Liberman, *J. Chem. Phys.*, **53**, 1891–1898 (1970).
(11) R. F. Stewart, E. R. Davidson, and W. T. Simpson, *J. Chem. Phys.*, **42**, 3175–3187 (1965).
(12) The secondary extinction correction is applied to F_c as $F_c/(1.0 + \text{EXT1} \times \text{EXT2} \times \text{BO})$ (where EXT1 and EXT2 are the reflection intensity and the Zachariasen "β" factor, respectively, and BO is refined). For additional details, see W. H. Zachariasen, *Acta Crystallogr.*, **16**, 1139–1144 (1963).
(13) The formulas used in the reduction of X-ray intensity data follow: *Lp* (Lorentz-polarization factor) = $(\cos^2 2\theta + \cos^2 2\theta_m)/2 \sin 2\theta$, where θ and θ_m (13.25°) are the reflection and monochromator Bragg angles, respectively; I (net peak intensity) = $[CT - (t_p/t_b)(B_1 + B_2)]$, where CT is the total peak count in t_p s and B_1 and B_2 are the individual background counts in $(t_b/2)$ s; $\sigma(I)$ (reflection esd) = $[CT + (t_p/t_b)^2 (B_1 + B_2)]^{1/2}$; $\sigma(F_o)$ (weighted reflection esd) = $\frac{1}{2}[\sigma(I)/Lp]^2 + (p|F_o|^2)^2]^{1/2}/2|F_o|$; $\sigma_s(F_o)$ (the reflection esd from counting statistics alone) = $\sigma(I)/2(Lp)(|F_o|)$; R_s (the statistical R factor) = $\Sigma\sigma_s(F_o)/\Sigma|F_o|$.
(14) The formula used to correct for anisotropic decay of reflection data is described by M. R. Churchill and K. L. Kalra, *Inorg. Chem.*, **13**, 1427–1437 (1974).
(15) For details of the analytical absorption correction method, see J. De Meulenaer and H. Tompa, *Acta Crystallogr.*, **19**, 1014–1018 (1965); P. Coppens and W. C. Hamilton, *Acta Crystallogr., Sect. A*, **26**, 71–83 (1970).
(16) C. K. Johnson, Report ORNL-3794, Oak Ridge National Laboratory, Oak Ridge, Tenn., 1965.
(17) W. R. Busing, K. O. Martin, and H. A. Levy, Report ORNL-TM-306, Oak Ridge National Laboratory, Oak Ridge, Tenn., 1962.
(18) D. M. Blow, *Acta Crystallogr.*, **13**, 168 (1960).
(19) *Chem. Soc., Spec. Publ.*, **No. 18** (1965): (a) p S14s; (b) p S15s.
(20) M. Ehrenberg, *Acta Crystallogr.*, **20**, 177–182 (1966).
(21) J. Gaultier, C. Hauw, J. P. Desvergne, and R. Lapougade, *Cryst. Struct. Commun.*, **4**, 497–500 (1975).
(22) D. J. Cram and J. M. Cram, *Acc. Chem. Res.*, **4**, 204–213 (1971).
(23) D. A. Buckingham, P. J. Cresswell, R. J. Dellaca, M. Dwyer, G. J. Gainsford, L. G. Marzilli, I. E. Maxwell, W. T. Robinson, A. M. Sargeson, and K. R. Turnbull, *J. Am. Chem. Soc.*, **96**, 1713–1725 (1974).
(24) R. H. Boyd, *J. Chem. Phys.*, **49**, 2574–2583 (1968).
(25) J. Ferguson and M. Puza, *Chem. Phys. Lett.*, **53**, 215–218 (1978).
(26) J. Ferguson, A. W-H. Mau, and J. M. Morris, *Aust. J. Chem.*, **26**, 91–102 (1973).
(27) J. Ferguson, A. W-H. Mau, and M. Puza, *Mol. Phys.*, **21**, 1457–1466 (1974).
(28) H. Beens and A. Weller, "Organic Molecular Photophysics," Vol. 2, J. B. Birks, Ed., Wiley, New York, 1975, pp 159–215.
(29) Please refer to the table in supplementary material.